Magnetic-field-induced color change in α-Fe_2O_3 single crystals

P. Chen,[1] N. Lee,[2] S. McGill,[3] S.-W. Cheong,[2] and J. L. Musfeldt[1,*]

[1]*Department of Chemistry, University of Tennessee, Knoxville, Tennessee 37996, USA*

[2]*Rutgers Center for Emergent Materials and Department of Physics and Astronomy, Rutgers University, Piscataway, New Jersey 08854, USA*

[3]*National High Magnetic Field Laboratory, Tallahassee, Florida 32310, USA*

(Received 18 October 2011; published 10 May 2012)

We investigated the magneto-optical properties of α-Fe_2O_3 in order to understand the interplay between charge and magnetism in a model transition metal oxide. We discovered that hematite appears more red in applied magnetic field than in zero-field conditions, an effect that is amplified by the presence of the spin-flop transition. Analysis of the exciton pattern on the edge of the *d*-*d* color band reveals $C2$ monoclinic symmetry in the high-field phase. These findings advance our understanding of magnetoelectric coupling away from the static limit and motivate spectroscopic work on other iron-based materials under extreme conditions.

DOI: 10.1103/PhysRevB.85.174413 PACS number(s): 78.20.Ls, 75.30.Ds, 75.50.Ee, 78.20.Bh

The interplay between charge, structure, and magnetism is at the heart of the rich tunability in transition metal oxides.[1–3] Color properties in particular reveal crystal field environments and electronic transition around and between metal centers.[4,5] At the same time, the optical properties of a material often display collective excitations like excitons and magnon sidebands. They are induced by exchange coupling and therefore very sensitive to variations in magnetic order.[6,7] When combined with external stimuli like temperature or magnetic field, optical spectroscopy can reveal transition mechanisms, local symmetry breaking, and microscopic insight into fundamental mixing processes.[8–10] In this work, we focus on α-Fe_2O_3, a model antiferromagnet with large exchange couplings and experimentally realizable critical fields[11–13] and the parent compound from which other functional oxides (like multiferroic $BiFeO_3$ and $LuFe_2O_4$) derive.

α-Fe_2O_3 is commonly known as hematite.[14] It crystallizes in the rhombohedral corundum structure ($R\bar{3}c$) at ambient conditions.[15] The system is antiferromagnetic below the 260 K Morin transition (T_M),[16] with spins lying along the [111] axis of the trigonal unit cell [inset, Fig. 1(a)]. Both temperature (T_M) and magnetic field ($B_{C\parallel} = 6.8$ T, $B_{C\perp} = 16.0$ T)[12,13,17] drive a spin flop to the basal plane,[18] and in the high temperature/field phase, α-Fe_2O_3 is weakly ferromagnetic due to a slight ($\sim 10^{-4}$ degree) spin canting.[19,20] Previous spectroscopic work revealed the electronic structure and identified the exciton and associated magnon sideband on the leading edge of the ${}^6A_{1g} \rightarrow {}^4T_{1g}$ on-site excitation.[21,22] No exciton fine structure was resolved, which prevented an analysis of magnetic symmetry, and magnetic field effects in this iconic material have not been explored from an optical properties point of view.

Here we report the discovery that applied magnetic field drives a color change in α-Fe_2O_3 such that it appears more red in the high field phase. This chameleonic effect arises because the Fe^{3+} on-site excitations are intrinsically coupled to magnetic ordering. Spin-orbit coupling naturally mixes charge and spin excitations,[23] but the effect is amplified here by the presence of the spin flop transition. Analysis of the exciton pattern superimposed on the color band reveals $C2$ monoclinic symmetry in the high field phase, providing a powerful and general illustration of how this type of analysis can be used for magnetic symmetry determination in the absence of neutron data. The discovery of magnetochromism in this model system extends our understanding of charge-spin coupling in iron-based solids[8,24–26] and the functional oxides that derive from hematite, and it provides a strategy for the development of next-generation magneto-optical materials. This strategy recommends incorporation of collective magnetic transitions in intrinsically colored compounds.

High-quality α-Fe_2O_3 single crystals were grown using the flux method. Most work on hematite has been carried out on samples of mineralogical origin, so the preparation of large crystals with high purity provides additional motivation for this work. X-ray shows no impurity phases and a single oxidation state. We employed five independent crystals of varying thicknesses and either (111) or ($\bar{1}10$) orientation for our optical properties work.[28] This combination allowed us to obtain complete results over the full frequency range of interest and optimal sensitivity to the small features on the leading edge of the ${}^6A_{1g} \rightarrow {}^4T_{1g}$ on-site excitation. Spectra were collected using a Bruker Equinox 55 Fourier transform infrared spectrometer equipped with a microscope attachment (600–17 000 cm^{-1}). Temperature control was achieved with an open-flow cryostat. Magneto-optical measurements (0.1 cm^{-1} resolution) were carried out at the NHMFL using the 35 T resistive magnet system ($B \parallel [111]$, $B \perp [111]$). We calculated the optical constants using a Glover-Tinkham analysis.[31,32] Traditional peak fitting and group theoretical methods were employed as appropriate. The magnon density of states was calculated numerically.[28]

Figure 1(a) displays the optical response of α-Fe_2O_3. We assign the two strong, broad bands centered at $\sim$11 550 and 15 300 cm^{-1} as ${}^6A_{1g} \rightarrow {}^4T_{1g}$ and ${}^6A_{1g} \rightarrow {}^4T_{2g}$ on-site excitations.[21,22] These *d*-*d* excitations are formally forbidden although they appear in many oxides due to spin-orbit coupling, exchange interaction, and odd parity phonons that hybridize states and break inversion symmetry.[9,21,35] Low temperature reveals a great deal of fine structure on the leading edge of the ${}^6A_{1g} \rightarrow {}^4T_{1g}$ band [Fig. 1(b)]. These strongly polarized features are collective excitations. Their properties are summarized in Table I. For the purposes of our discussion, the fundamental magnetic- and electronic-dipole excitations, $M1$ and $E1$, are most important. Interactions between four

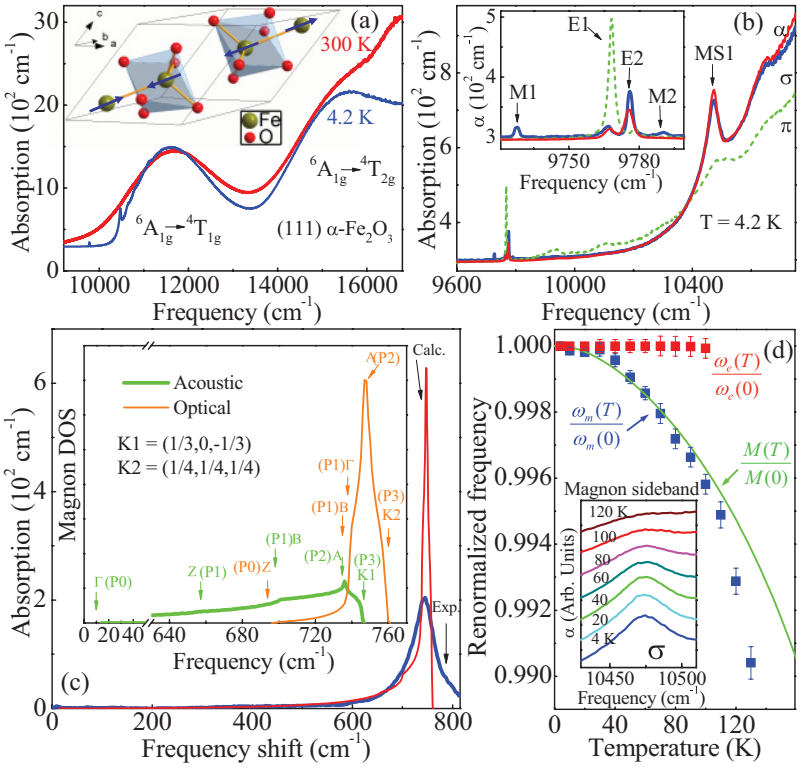

FIG. 1. (Color online) (a) Absorption coefficient, $\alpha(\omega)$, of α-Fe_2O_3 in the range of on-site Fe^{3+} d-d excitations at 300 and 4.2 K. Inset: rhombohedral lattice[27] and low temperature four sublattice spin structure.[18] (b) Close up view of the fine structure on the leading edge of the $^6A_{1g} \rightarrow {}^4T_{1g}$ on-site excitation at 4.2 K in the α, σ, and π polarizations. Inset: close-up view of the excitons. (c) Comparison of the σ-polarized magnon sideband absorption spectrum with the calculated density of states. Inset: Calculated magnon density of states using optimized exchange constants $J_1 = 7.6$ K, $J_2 = 2.0$ K, $J_3 = -27.7$ K, and $J_4 = -22.2$ K.[28] The frequency channel width was taken to be 1 cm^{-1}. The nature of the critical points in Brillouin zone are indicated.[29] (d) Temperature dependence of $E1$ (π) exciton and magnon sideband (MS1, α) peak positions, expressed as the ratio of $\frac{\omega_e(T)}{\omega_e(0)}$ and $\frac{\omega_m(T)}{\omega_m(0)}$, respectively. The latter compares well with the calculated sublattice magnetization[11,30] using the same exchange constants listed above. Inset: $\alpha(\omega)$ of the σ-polarized magnon sideband at different temperatures.

translationally inequivalent Fe^{3+} sites in the magnetic structure give rise to Davydov splitting between the ($M1\sigma$, $E1\pi$) and ($M2\sigma$, $E2\pi$) exciton pairs.[28] These splittings are 38.6 and 14.0 cm^{-1}, respectively, an order of magnitude larger than in $YCrO_3$ (2 cm^{-1})[36] and Cr_2O_3 (3.5 cm^{-1}).[37] This is a consequence of the larger inter-sublattice coupling energy in α-Fe_2O_3. The feature labeled MS1 is assigned as the magnon sideband.[22] Based on the position, shape, and polarization behavior, we associate it with the $M1\sigma$ exciton.[38] The intensity is stronger than that of $M1\sigma$ because this electric dipole-allowed excitation involves pairs of ions and thus breaks the parity selection rule.[9,39] The magnon sideband frequency can be expressed as $\omega = \omega_e + \omega_m$,[40] where ω_e is the exciton frequency, and ω_m is the magnon frequency. We find $\omega_m = 743.7 \pm 0.1$ cm^{-1} in excellent agreement with the magnon energy obtained by neutron scattering.[11] Other collective excitations including phonon sidebands and the two magnon sideband are also observed.[28]

TABLE I. Properties of $^6A_{1g} \rightarrow {}^4T_{1g}$ fine structure in α-Fe_2O_3 at 4.2 K. In the line notation, M represents magnetic dipole character, E is electric dipole, and MS is magnon sideband. In the polarization notation, α ($\widetilde{E} \perp c, \widetilde{B} \perp c$), σ ($\widetilde{E} \perp c, \widetilde{B} \parallel c$), π ($\widetilde{E} \parallel c, \widetilde{B} \perp c$), $\widetilde{E}$ and $\widetilde{B}$ are the electric and magnetic vector of light, c is [111] axis of the crystal. $f \equiv \frac{2c}{N_e \pi \omega_p^2} \int_{\omega_1}^{\omega_2} n\alpha(\omega, B)\, d\omega$, here, $N_e = 5$ is the number of electrons per Fe site, $n \simeq 2.23$ is the refractive index, ω_p is the plasma frequency $\equiv \sqrt{\frac{e^2\rho}{m\epsilon_0}}$, e and m are the charge and mass of an electron, ϵ_0 is the vacuum dielectric constant, ρ is the density of Fe sites, c is the speed of light, ω_1 and ω_2 are the frequency limits of integration.[33]

Line	Polarization	Position (cm^{-1})	f 10^{-10}	Representation C_3	Representation R$\bar{3}$C
$M1$	σ	9727.9	4.8	A	Γ_2^+
$E1$	π	9766.4	80	A	Γ_2^{-34}
	α, σ		8.6	C_1/C_2	Γ_3^-
$E2$	π	9776.1	4.3	A	Γ_2^{-34}
	α, σ		23	C_1/C_2	Γ_3^-
$M2$	σ	9790.1	2.5	A	Γ_2^+
MS1	α, σ, π	10471.5	1400		

We analyzed the magnon sideband selection rules[41] at different points in the Brillioun zone and calculated the density of states using the magnon dispersion of Samuelsen.[28,42] The results are in good agreement with the measured absorption spectrum [Fig. 1(c)] and explain the directionally-dependent magnon sideband shape.[28] The exciton and magnon features display characteristic temperature dependence. As shown in Fig. 1(d), expressing the magnon sideband frequency as $\frac{\omega_m(T)}{\omega_m(0)}$ reveals high temperature softening, whereas the reduced frequency of the $E1\pi$ exciton is relatively constant. The former compares well with a numerical calculation of the normalized sublattice magnetization ($\frac{M(T)}{M(0)}$) using the random phase approximation.[28] The discrepancy in the high temperature range is because magnetization measures the thermal average population of magnons and is less sensitive to the zone boundary (A point) dispersion.[40,43] Similar effects are observed in MnF_2[40] and Cr_2O_3.[10]

Figure 2(a) displays the field-induced absorption difference spectra of α-Fe_2O_3 for the α polarization and B $\parallel$ [111]. The magnetochromic response reveals that the on-site excitations are intrinsically coupled to the microscopic spin structure. We can quantify the field-induced color change with the partial sum rule [inset, Fig 2(a)].[33] Oscillator strength changes

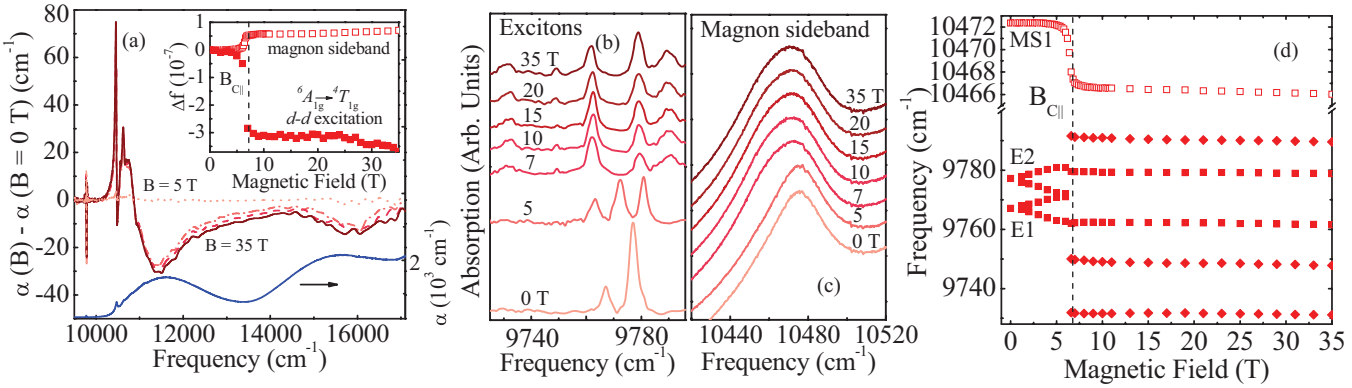

FIG. 2. (Color online) (a) Absorption difference spectra [α(B) - α(B = 0 T)] of α-Fe_2O_3 at 4.2 K for the α-polarization and B ∥ [111] at selected magnetic fields: 5, 10, 15, 35 T. The corresponding low temperature zero field absorption spectrum is shown as a blue solid curve for comparison. Inset: oscillator strength change in the range of the magnon sideband and $^6A_{1g} \rightarrow {}^4T_{1g}$ on-site excitation as a function of magnetic field. (b, c) Close-up view of the excitons and magnon sideband at selected fields. (d) Peak position vs. magnetic field for the exciton and magnon sideband features. Error bars of these positions are smaller than the symbol size and not shown.

(Δf) show a first order transition at $B_{C\parallel} = 6.6 \pm 0.2$ T when B ∥ [111], and a broad transition at $B_{C\perp} = 16.2 \pm 0.2$ T when B ⊥ [111].[28] These critical fields are easily assigned as field-induced spin flop transitions in agreement with magnetization[12] and ultrasonic attenuation measurements.[13] Importantly, the *d*-*d* on site excitations are in the visible range and responsible for the reddish color of α-Fe_2O_3. As shown in the absorption difference plot, this system absorbs fewer photons in the red color range in high magnetic field (on the order of 2% less, the maximum transmittance change is ∼16%[28]). α-Fe_2O_3 thus appears more red in the magnetically reoriented phase.[44] This color change is observed because the coherent spin transition amplifies the charge-spin interaction beyond what one might expect from traditional spin-orbit processes alone. The field-induced reduction of oscillator strength of the $^6A_{1g} \rightarrow {}^4T_{1g}$ band is partially recovered in the magnon sideband [inset, Fig. 2(a)]. Optical property changes driven by magnetic order reorientation have been observed in other functional materials including $FeCO_3$ (color contrast at the 13 T spin-flop transition due to a "double" magnon sideband mechanism)[6] and $BiFeO_3$ (color change at 20 T due to shifted magnon sideband excitations caused by spin spiral quenching).[8] Here, we report the discovery of such an effect in α-Fe_2O_3, although it occurs by a fundamentally different mechanism.

Magnon sideband formation is controlled by exchange coupled pairs,[39,45] and as a consequence, field-induced magnetic order reorientation will significantly impact the behavior. Strikingly, the magnon sideband displays a 27% increase in oscillator strength at 35 T compared to its zero-field value [inset, Fig. 2(a)].[28] Magnon sideband intensity is dependent upon (i) exciton + magnon joint density of states and (ii) collinearity of the magnetic structure.[6,7] It will decrease dramatically if spin collinearity is violated as in $RbMnF_3$[7] and $FeCO_3$.[6] Based on the observed intensity increase, we conclude that spin collinearity is, for all practical purposes, conserved through the spin-flop transition in α-Fe_2O_3.[46]

Figure 2(c) shows a close-up view of the magnon sideband excitation at selected magnetic fields. The field-induced frequency shifts are summarized in Fig. 2(d), and like the oscillator strength, place the critical spin-flop fields at $B_{C\parallel} = 6.6 \pm 0.2$ T and $B_{C\perp} = 16.2 \pm 0.2$ T.[28] Importantly, the magnon sideband softens by ∼6 cm^{-1} through the 6.6 T transition. Assuming that the magnon dispersion does not change substantially,[42] we can estimate changes in the exchange constants ($\frac{\Delta J}{J}$) using a least squares fit of the magnon density of states to the 35 T σ-polarized spectrum.[28] The results show that ferromagnetic couplings J_1 and J_2 increase by ∼15% and 8%, respectively, whereas antiferromagnetic couplings $|J_3|$ and $|J_4|$ decrease by ∼1%. These results indicate larger direct exchange[11] and smaller superexchange in the high-field phase. These modified exchange interactions impact the electronic structure through spin-orbit processes.

Exciton behavior can be used to reveal magnetic symmetry in the high-field phase of α-Fe_2O_3. At $B_{C\parallel}$, the Zeeman splitting disappears, and a new pattern emerges [Fig. 2(d)].

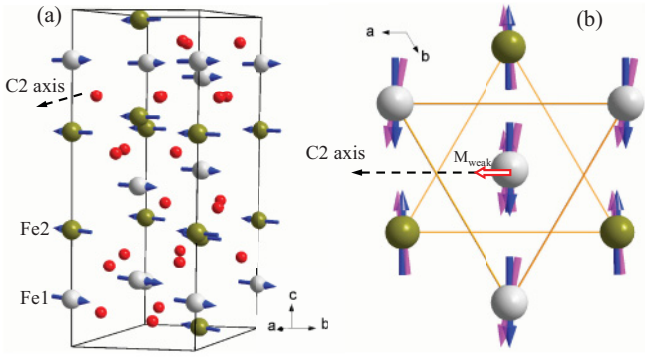

FIG. 3. (Color online) (a) Schematic view of the high temperature[18]/field magnetic structure of α-Fe_2O_3. The *C*2 rotational axis is indicated. (b) View of the magnetic ordering pattern looking down the [111] axis showing only the Fe centers. Blue arrows denote the collinear spin arrangement, and purple arrows schematically show the noncollinear state. The canting angle is on the order of ∼10^{-4} degrees and arises due to Dzyaloshinskii-Moriya interactions.[19,20] Canting induces a weak ferromagnetic moment M_{weak} along the direction of the *C*2 rotational axis (red arrow). This symmetry is clarified on the central Fe site, where the spin vector on the site of interest is shown along with that on the site below.

This more complicated exciton pattern arises from the transition to a different magnetic ordering. Above $B_{C\|}$, lower symmetry lifts the degeneracy of the $E1\alpha$ exciton and gives rise to a new peak at ~9748 cm^{-1}.[47] Two magnetic-dipole excitons, $M1\sigma$ and $M2\sigma$, are also activated due to the new coordinate system (and selection rules) above 6.2 T. $M1\sigma$ hardens by 4.6 cm^{-1}, whereas $M2\sigma$ softens by 0.5 cm^{-1}. To explore the symmetry of the high-field phase, we make use of the observed exciton pattern in the α, σ, and π polarizations[28] and invoke two additional constraints: (i) the new magnetic order symmetry must be either the same or a subgroup of the original $R\bar{3}c$ structure and (ii) spin collinearity is conserved above $B_{C\|}$. The latter is based upon the increase in magnon side-band intensity with field and requires that inversion and $C2$ rotational operations be maintained.

Several symmetry candidates emerge from this analysis.[48] They include $P1$, $P\bar{1}$, $C2$, Cc, $C2/c$, $R3$, $R\bar{3}$, $R32$, and $R3c$. Only the $C2/c$ monoclinic structure contains the necessary inversion center and $C2$ rotational axis and is consistent with our magneto-optical results (especially high field splitting of E1α). We thus infer that the field-induced magnetic ordering is monoclinic with $C2/c$ symmetry—at least to first order. We know, however, that weak canting due to the Dzyaloshinskii-Moriya effect formally eliminates the inversion center[19,20] [Fig. 3(a)]. This higher order effect places additional constrains on the system. Reevaluating the magnetic symmetry with the surviving $C2$ operation (and without the inversion center), we find that only the $C2$ monoclinic structure meets our criteria.[28] We therefore conclude that the formal symmetry of the field-induced ordered phase of α-Fe_2O_3 is $C2$. Switching the applied field to the (111) plane, the exciton pattern in the new magnetic order is consistent with the aforementioned group theory predictions for $C2/c$ or $C2$ magnetic symmetry (depending upon whether spin canting-induced symmetry breaking is ignored or invoked),[28] demonstrating that magnetic fields in different directions drive to identical high-field phases in α-Fe_2O_3.

Summarizing, we report the discovery of magnetochromism in one of the world's oldest and most iconic antiferromagnetic materials, α-Fe_2O_3. In addition to a field-induced color change due to the reorientation of magnetic order, the exciton pattern reveals $C2$ monoclinic symmetry in the high-field phase. This work advances our understanding of the interplay between charge and magnetism, identifies a strategy for the development of next-generation color change materials, and motivates fundamental research on other iron-based materials under extreme conditions and away from the static limit.

This work was supported by the Materials Science Division, Basic Energy Sciences, US Department of Energy [Contract Nos. DE-FG02-01ER45885 at UT (J.L.M.) and DE-FG02-07ER46382 at Rutgers University (S.W.C.)] and the National Science Foundation [DMR-0654118 at the NHMFL (S.M.G.)].

*Corresponding author.

[1] M. Imada, A. Fujimori, and Y. Tokura, Rev. Mod. Phys. **70**, 1039 (1998).
[2] S. A. Kivelson, E. Fradkin, and V. J. Emery, Nature (London) **393**, 550 (1998).
[3] S. W. Cheong and M. Mostovoy, Nat. Mater. **6**, 13 (2007).
[4] F. J. Kahn, P. S. Pershan, and J. P. Remeika, Phys. Rev. **186**, 891 (1969).
[5] T. Arima, Y. Tokura, and J. B. Torrance, Phys. Rev. B **48**, 17006 (1993).
[6] V. V. Eremenko, Yu. G. Litvinenko, and V. I. Myatlik, JETP Lett.-USSR **12**, 47 (1970).
[7] V. V. Eremenko and E. G. Petrov, Adv. Phys. **26**, 31 (1977).
[8] X. S. Xu *et al.*, Phys. Rev. B **79**, 134425 (2009).
[9] D. D. Sell, R. L. Greene, and R. M. White, Phys. Rev. **158**, 489 (1967).
[10] J. W. Allen, R. M. Macfarlane, and R. L. White, Phys. Rev. **179**, 523 (1969).
[11] E. J. Samuelsen and G. Shirane, Phys. Status Solidi **42**, 241 (1970).
[12] S. Foner and Y. Shapira, Phys. Lett. A **29**, 276 (1969).
[13] Y. Shapira, Phys. Rev. **184**, 589 (1969).
[14] Hematite means "blood" in Greek and refers to the red color of the powdered mineral. This iconic material has been used for thousands of years in amulets and pigments and as the main source of elemental iron, and plays a central role in corrosion problems (as the main component of rust).
[15] L. Pauling and S. B. Hendricks, J. Am. Chem. Soc. **47**, 781 (1925).
[16] F. J. Morin, Phys. Rev. **78**, 819 (1950).
[17] T. Kaneko and S. Abe, J. Phys. Soc. Japan **20**, 2001 (1965).
[18] C. G. Shull, W. A. Strauser, and E. O. Wollan, Phys. Rev. **83**, 333 (1951).
[19] I. Dzyaloshinsky, J. Phys. Chem. Solids **4**, 241 (1958).
[20] T. Moriya, Phys. Rev. **120**, 91 (1960).
[21] L. A. Marusak, R. Messier, and W. B. White, J. Phys. Chem. Solids **41**, 981 (1980).
[22] A. I. Galuza, A. B. Beznosov, and V. V. Eremenko, Low Temp. Phys. **24**, 726 (1998).
[23] Large spin-orbit coupling is not expected in Fe^{3+}. The color change is observed in α-Fe_2O_3 because of the collective transition.
[24] X. S. Xu *et al.*, Phys. Rev. Lett. **101**, 227602 (2008).
[25] W. F. J. Fontijn *et al.*, J. Appl. Phys. **85**, 5100 (1999).
[26] L. V. Gasparov, D. B. Tanner, D. B. Romero, H. Berger, G. Margaritondo, and L. Forro, Phys. Rev. B **62**, 7939 (2000).
[27] L. W. Finger and R. M. Hazen, J. Appl. Phys. **51**, 5362 (1980).
[28] See Supplemental Material at http://link.aps.org/supplemental/10.1103/PhysRevB.85.174413 for details.
[29] J. C. Phillips, Phys. Rev. **104**, 1263 (1956).
[30] R. E. Mills, R. P. Kenan, and F. J. Milford, Phys. Rev. **145**, 704 (1966).
[31] P. Chen *et al.*, Appl. Phys. Lett. **96**, 131907 (2010).
[32] M. Tinkham, in *Far Infrared Properties of Solids*, edited by S. S. Mitra and S. Nudelman (Plenum, New York, 1970).
[33] F. Wooten, *Optical Properties of Solids* (Academic Press, New York, 1972).
[34] This assignment relies on the similar intensity of excitons in α and σ polarizations and magnetic field results.
[35] L. L. Lohr, Coord. Chem. Rev. **8**, 241 (1972).
[36] K. Aoyagi, K. Tsushima, and S. Sugano, Solid State Commun. **7**, 229 (1969).
[37] J. P. van der Ziel, Phys. Rev. Lett. **18**, 237 (1967).
[38] The intensity of MS1 increases as that of $M1\sigma$ when rotating the polarizer from the π to σ direction.

[39]J. W. Halley and I. Silvera, Phys. Rev. Lett. **15**, 654 (1965).
[40]R. L. Greene *et al*., Phys. Rev. Lett. **15**, 656 (1965).
[41]M. Lax and J. J. Hopfield, Phys. Rev. **124**, 115 (1961).
[42]E. J. Samuelsen, Physica **43**, 353 (1969).
[43]N. W. Ashcroft and N. D. Mermin, *Solid State Physics* (Brooks Cole, Pacific Grove, 1976).
[44]Our data reveal that temperature and magnetic-field effects in α-Fe_2O_3 are quite different. The color change through the temperature-driven spin-flop transition[21] is entangled with phonon-assisted trends that grow with temperature. Moreover, the signature of the spin flop transition is small compared with the rising phonon-assisted background, and it has an opposite trend, making changes difficult to discern. Finally, exciton and magnon sideband peaks can not be observed above 150 K. As we show here, these peaks are incredibly sensitive to variations in magnetic order. This makes optical properties work through the field-driven spin-flop transition the preferred strategy for investigating ordering-induced color change and mechanistic issues.
[45]Y. Tanabe, T. Moriya, and S. Sugano, Phys. Rev. Lett. **15**, 1023 (1965).
[46]Above B_C, the spins cant toward each other by a small angle (on the order of 10^{-4} degrees) due to Dzyaloshinskii-Moriya interactions.[19,20] As we shall see, this higher order effect eliminates the inversion center and formally reduces the symmetry of the field-induced magnetically-ordered phase from $C2/c$ to $C2$.
[47]An additional peak should split from $E2\alpha$ but is not observed, probably because it is superimposed with $E1\alpha$.
[48]C. Hermann, Z. Kristallogr. **89**, 32 (1934).